دراسة تاثير التلدين على الخواص التركيبية والبصرية لأغشية SnO_2 الرقيقة النانوية المحضرة بتقنية الرش الحراري

د. رضية مهدي شاكر الجراح* نور علي جعفر**
جامعة الكوفة – كلية العلوم – قسم الفيزياء

Study the Effect of Annealing on the Structural and Optical Properties of Nano SnO_2 Thin Films Prepared by Spray Pyrolysis Technical

Radhiyah Mahdi Shaker al jarrah* **Noor Ali Jaafer****
University of Kufa - Faculty of Science - Department of Physics
***Email: radhiyah.aljarrah@uokufa.edu.iq,**
**** noor.ajaafer@gmail.com**

Abstract

In this work, the effect of annealing temperature T_a on the structural and optical properties of SnO_2 nanostructure prepared by spray pyrolysis method was investigated. SnO_2 films prepared on glass substrate with thickness 250 nm by dissolved 2.2563 g of $SnCl_2.2H_2O$ in 100 ml of ethanol then added 60 drops from concentrated hydrochloric acid (HCl).

After that the films were annealed at various temperatures (573, 673 and 773 K). X-ray diffraction studies show that the structure of all SnO_2 films is polycrystalline with tetragonal rutile crystalline structure with preferential orientation in the (200) direction.

The optical measurement showed that the nature of the optical transition has been direct with average band gap energies have tendency to decreases from 3.98 eV to 3.73 eV with increasing of T_a. The extent and nature of transmittance and optimized band gap of the material assure to utilize it for photovoltaic applications.

Keywords: Annealing; Band gap; grain size; Spray pyrolysis; tetragonal; transmittance

الخلاصة:

في هدا العمل تم استقصاء تأثير درجة حرارة التلدين على الخواص التركيبية والبصرية لمادة SnO_2 النانوية التركيب المحضرة بطريقة الرش الحراري. حُضرت أغشية SnO_2 على ركائز من الزجاج بسمك 250 نانوميتر وذلك باذابة 2.2563 غرام من مادة $SnCl_2.2H_2O$ في 100 مل من كحول الايثانول بعدها تم إضافة 60 قطرة من حامض الهيدروكلويك (HCl).بعدها تم تلدين الأغشية لمختلف الدرجات الحرارية .(573, 673 and 773 K).

دراسة حيود الأشعة السينية بينت بان تركيب جميع أغشية SnO_2 متعدد البلورات ذات تركيب بلوري نوع رباعي الإضلاع يتمحور بالاتجاه (101).

بينت قياسات الخواص البصرية بان طبيعة الانتقالات البصرية مباشرة مع معدل قيم فجوة الطاقة تميل للنقصان من 3.98 إلكترون فولت إلى 3.73 إلكترون فولت مع زيادة درجة حرارة التلدين.

حجم البلورات التي حصلنا عليها وطبيعة الانتقالات وقيم فجوة الطاقة للمادة قيم مناسبة لاستخدام المادة في التطبيقات الفوتوفولطائية.

الكلمات المفتاحية: التلدين, فجوة الطاقة, حجم الحبيبات, الرش الحراري, رباعي الاضلاع, النفاذية

1. Introduction

The thin film physics is one of the most important physics branch that deals with system of very small thickness it's from ten nanometer to a few micrometer [1, 2]. Thin films technology that play important place in the semiconductor application, It gave a clear idea of many of its physical properties [3].

Tin dioxide has been extensively studied for a long time for use as transparent oxide films in optoelectronic devices such as sensor, solar cells, liquid crystal displays (LCD), photo catalysis, lithium ion batteries, wastewater treatment, and large area flat panel displays.The SnO_2 thin films can be doped with a wide variety of transition metal ions to meet the demands of these many practical applications [4-8].

SnO_2 is n-type semiconductor with large exciton binding energy, wide and direct band gap and high carrier mobility [9]. Over time, SnO_2 has proven to be the most commonly used semiconductor oxide gas sensor that can detect a wide range of pollutant gases [10]. And it is inexpensive, non-toxic, and can be fabricated via simple processes [11].

SnO_2 films have been fabricated using various technologies, including sputtering, chemical vapor deposition CVD [12], spray pyrolysis , atomic layer deposition (ALD), pulsed laser deposition (PLD), physical vapor deposition (PVD), sol-gel, spray pyrolysis [13-15] and Chemical bath deposition (CBD) [12]. In this study tin dioxide thin films were prepared by the spray pyrolysis technique, the spray pyrolysis technique is particularly attractive because of its simplicity, fast, inexpensive, vacuumless and suitable for mass production.

2. Aim of the work

The purpose of this work is to finding the best temperature for creation of SnO_2 film and research of their figure of merits characteristics.

3. Experimental Procedure

Nanostructure SnO_2 film was fabricated by spraying 0.1 M concentration of tin salt solution on glass substrate at temperature of 450 ^oC, The solution was prepared by solving 2.2563 g of $SnCl_2.2H_2O$ was dissolved in 100 ml of ethanol then added 60 drope from concentrated hydrochloric acid (HCl) by using drop by drop technique the solution put on magnetic stirrer for 30 minits. The addition of HCl rendered the solution transparent, microscope glass slides, cleaned with HCL, distilled water solvents, and then put in uletra sonic cleaner for 15 mints.after that put it in ethanol and distilled water solvent and again put in uletrasonic cleaner for 15 mints, finally the substrates put in 100 ml of distilled water and eject it then let it dry. The spray rate of the solution was adjusted to be one sprinkling in a minute and the sprinkling time was about 10 seconds. The normalized distance between the spray nozzle and the substrate was 30 cm. SnO_2 films were treated thermally at different temperatures (573,673, and 773) K for two hours in air.

The thickness of the films (t) was determined using the weighing-method as shown in the following equation:

$$t = \frac{\Delta m}{\rho A} \ldots\ldots (1)$$

where Δm represents the mass difference of slide after and before the deposition, A represents the area of the film and ρ is the mass density, the thickness of the films prepared about 250 nm.

The structure of the films was examined by X-Ray Diffraction (XRD) using a Philips X-ray diffractometer system which records the intensity as a function of Bragg's angle. The source of radiation was Cu (kα) with wavelength λ=1.5406 Å, the current was 30 mA and the voltage was 40 kV. The scanning angle 2θ was varied in the range of 20°-60°

Atomic Force Microscope (AFM), (AA3000 Scanning Probe Microscope SPM, tip NSC35/AIBS) shown in photo plate 3.5 from Angstrom Advance Inc. tests were employed to examine the surface morphology.

The transmittance and absorbance of the films was measured using UV-VIS spectrophotometer Shimadzu UV/ Visible recorder spectrometer model 12600 in the spectral range 200-1100 nm.

The intensity of light (I) after crossing thickness of material x in an isotropic medium can be estimated by [16]:

$$I = I_o \exp(-\alpha x) \ldots\ldots\ldots (2)$$

where I_o is the initial intensity.

4. Results and discussion

The results of XRD tests for SnO_2 thin film deposit on glass substrate shown in figure (1), which indicates that, the structure of the films polycrystalline.

It is known that tin dioxide SnO_2 has a tetragonal rutile crystalline structure [17]. The unit cell consists of two metal atoms and four oxygen atoms. Each metal atom is situated amidst six oxygen atoms which approximately form the corners of a regular octahedron. Oxygen atoms are surrounded by three tin atoms which approximate the corners of an equilateral triangle.

The major diffraction peaks of some lattice planes can be indexed to the tetragonal unit cell structure of SnO_2 with lattice constants a = 4.71 Å and c= 3.19 Å, which are consistent with the standard values for bulk SnO_2 (JCPDS-041-1445, card No. 96-900-9083) [17]. There are six apparent peaks with 2θ values of (26.58 °, 33.8°, 37.87°, 51.64°, 61.7 and 65.7) corresponding to SnO_2 crystal planes peaks of (110), (101), (200), (211), (310), and (301) respectively.

The crystallite reveals the nano size and the d space which determined from Scherer's formula equation (3) and Bragg equation equation (4) [18] respectively are listed in table (1).

$$D = \frac{0.9\lambda}{\beta \cos\theta} \ldots\ldots(3)$$

$$n\lambda = 2d \sin\theta \ldots\ldots\ldots(4)$$

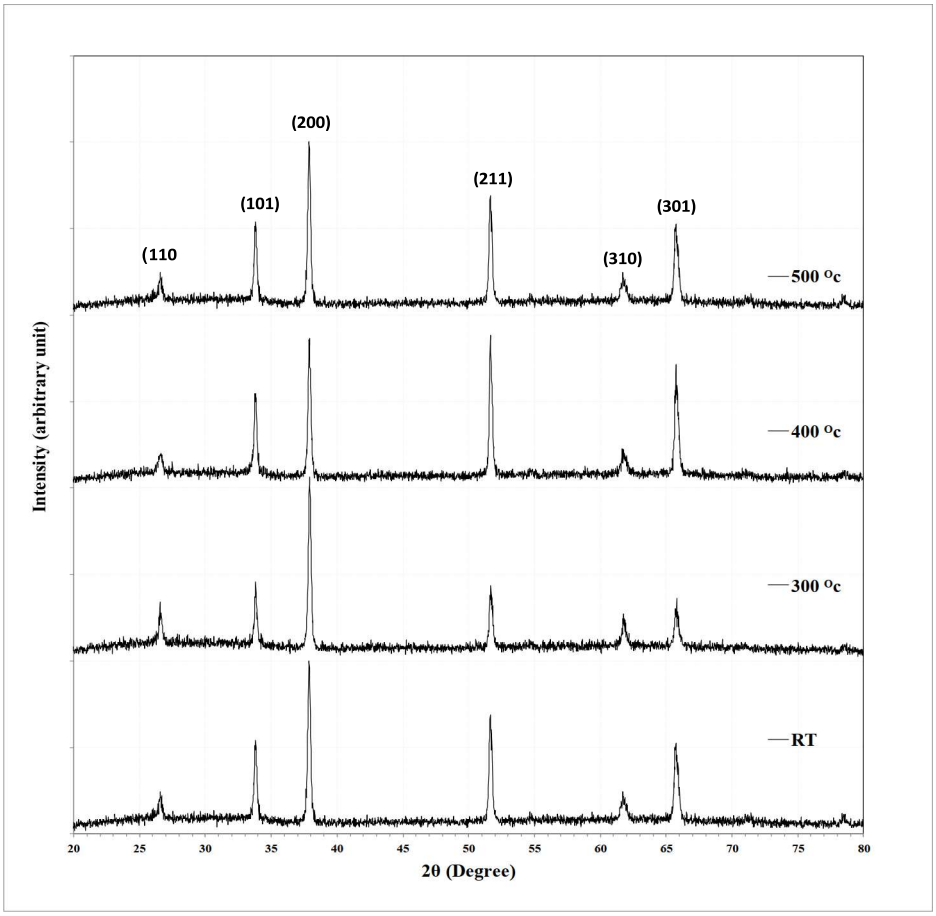

Fig.(1): X-ray diffraction (XRD) pattern of SnO_2 thin film at different annealing temperatures.

Table (1) Experimental and stander XRD data for SnO_2 films at different annealing temperatures.

T (^oC)	2θ (Deg.)	FWHM (Deg.)	d_{hkl} Exp.(Å)	G.S (nm)	d_{hkl} Std.(Å)	hkl
RT	26.5682	0.2749	3.3523	29.7	3.3498	(110)
	33.8086	0.2342	2.6491	35.5	2.6439	(101)
	37.8717	0.2749	2.3737	30.6	2.3686	(200)
	51.6395	0.2953	1.7686	29.9	1.7642	(211)
	61.7006	0.4481	1.5022	20.7	1.4981	(310)
	65.7026	0.3666	1.4200	25.8	1.4149	(301)
300	26.5479	0.2647	3.3549	30.8	3.3498	(110)
	33.8289	0.2443	2.6476	34.0	2.6439	(101)
	37.9226	0.2749	2.3707	30.6	2.3686	(200)
	51.6904	0.3359	1.7670	26.3	1.7642	(211)
	61.7821	0.2851	1.5004	32.5	1.4981	(310)
	65.7943	0.3768	1.4183	25.1	1.4149	(301)
400	26.5886	0.3462	3.3498	23.6	3.3498	(110)
	33.8086	0.2241	2.6491	37.1	2.6439	(101)
	37.9124	0.2545	2.3713	33.0	2.3686	(200)
	51.6497	0.2749	1.7683	32.1	1.7642	(211)
	61.7312	0.3462	1.5015	26.7	1.4981	(310)
	65.7332	0.3462	1.4194	27.3	1.4149	(301)
500	26.5580	0.2546	3.3536	32.1	3.3498	(110)
	33.8086	0.2545	2.6491	32.6	2.6439	(101)
	37.8717	0.2749	2.3737	30.6	2.3686	(200)
	51.6293	0.2953	1.7689	29.9	1.7642	(211)
	61.7108	0.3768	1.5019	24.6	1.4981	(310)
	65.7332	0.3767	1.4194	25.1	1.4149	(301)

Figure (2) shows surface morphologies of SnO_2 nanostructures. It can be seen that films are extremely smooth with RMS surface roughness of less than 3nm. The surface morphology as in figure is shown there are uniform distribution of homogeneous with columnar grains and an increasing in the grain size with annealing. The estimated grain size of the films is in the range of (57.6 – 68.8) nm. The average surface roughness, (RMS) values and the average surface grain size are listed in Table (2).

Table (2): Average crystallite size and roughness for as deposited and annealed SnO_2 thin films from AFM Images.

T_a (K)	**G.S (nm)**	**Root mean square(nm)**	**Roughness average (nm)**	**Peak-peak (nm)**
R.T	**57.6**	**1.6**	**1.23**	**7.1**
673	**62. 3**	**5. 9**	**4.04**	**21.5**
773	**64. 2**	**9. 5**	**8.15**	**23.7**
873	**68.8**	**3.4**	**3.12**	**12.1**

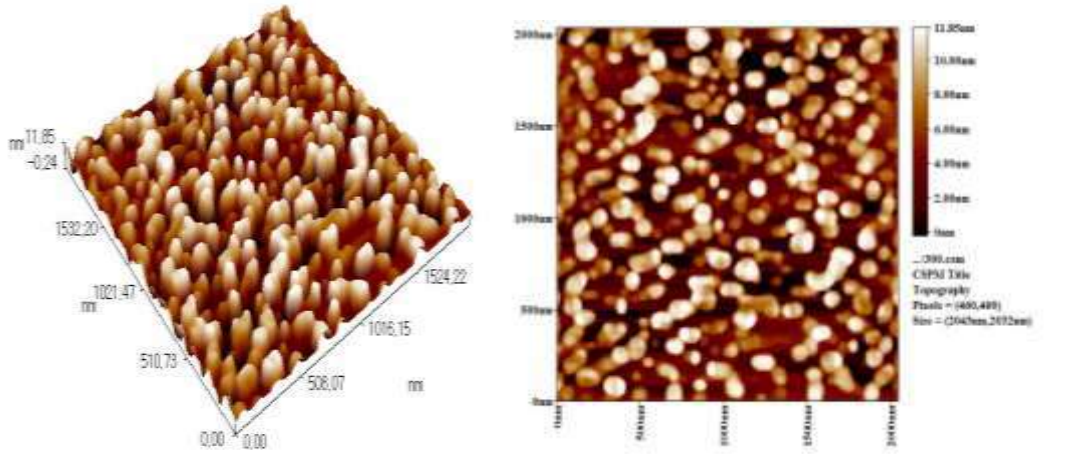

(a)

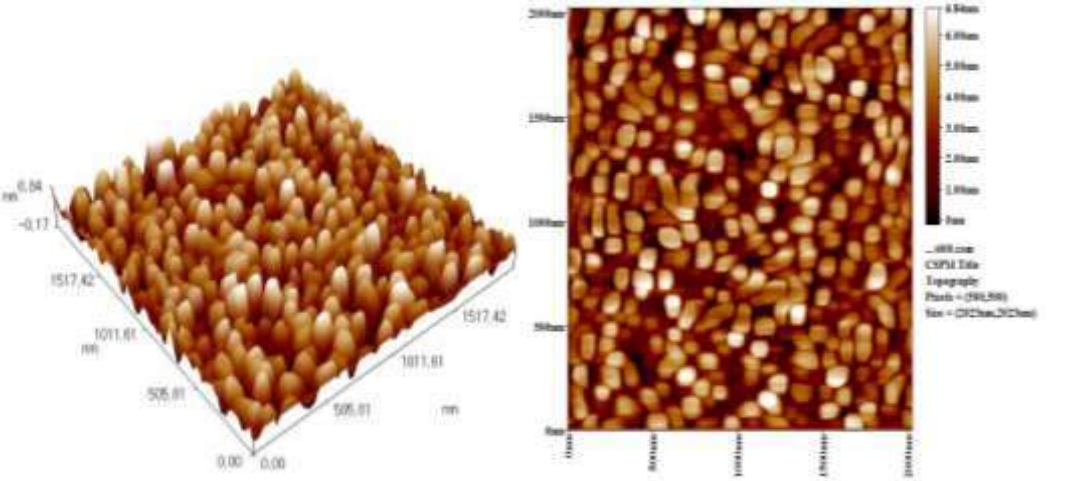

(b)

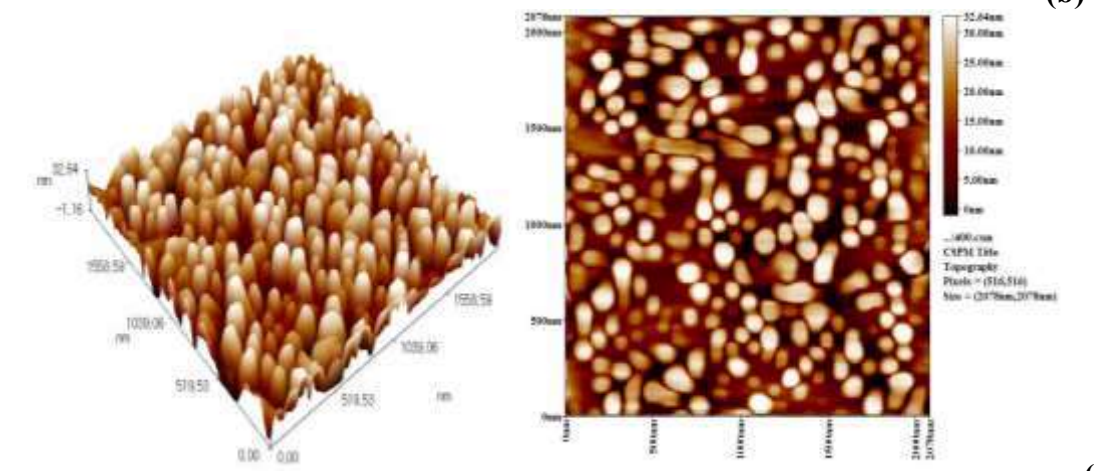

(c)

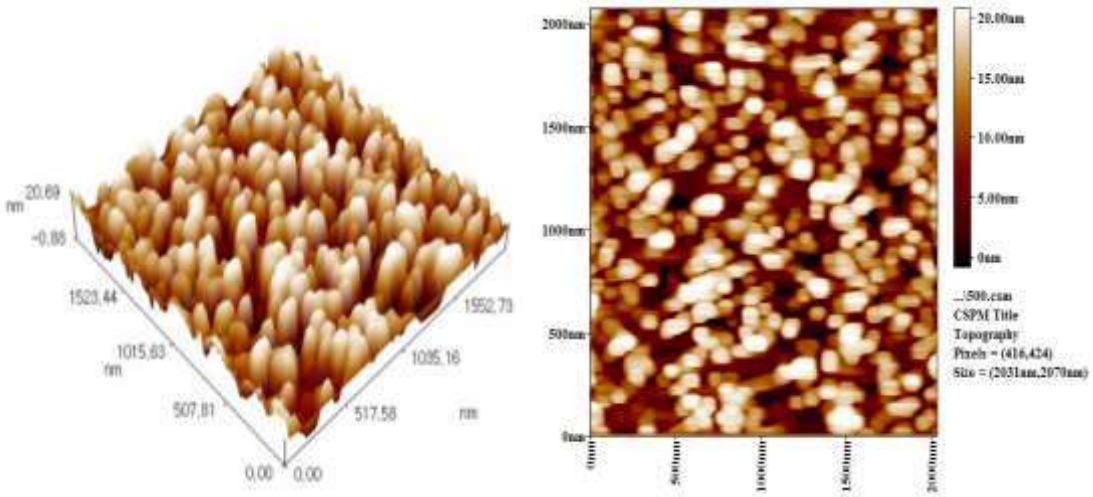

(d)

Fig.(2): AFM images;: at (a:R.T, b: Ta = 573 K ,c: Ta = 673 K, and d: Ta = 773K) of SnO_2 thin films.

The transmittances of SnO_2 films with different annealing conditions are shown in figure. (3). From this figure one can be seen clearly that the transmittance of SnO_2 above 85% for all films. Generally the required transmittance of transparent conductive thin film for solar cells and as such these results indicate that SnO_2 thin films are a good candidate to be used as a window layer in solar cells.

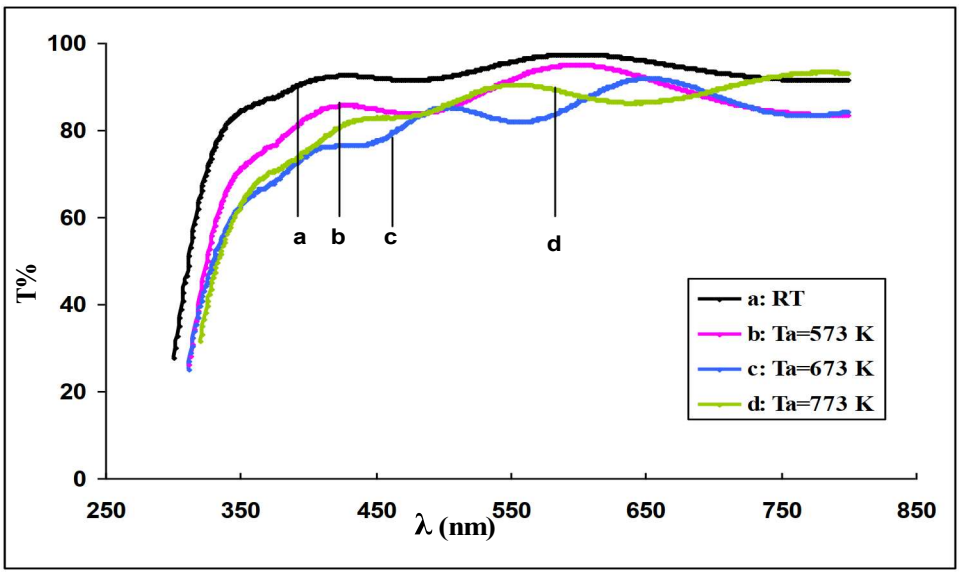

Fig. (3) Transmittance spectrum as a function of λ for SnO_2 film at different annealing temperatures.

Figure (4) shows refractive indices (n) values for SnO_2. The peak of refractive index at ~3.8 eV corresponds to direct band gap transition. The refractive index, in general changes slightly with increasing of annealing temperatures T_a and it is about 2.15 for all sample.

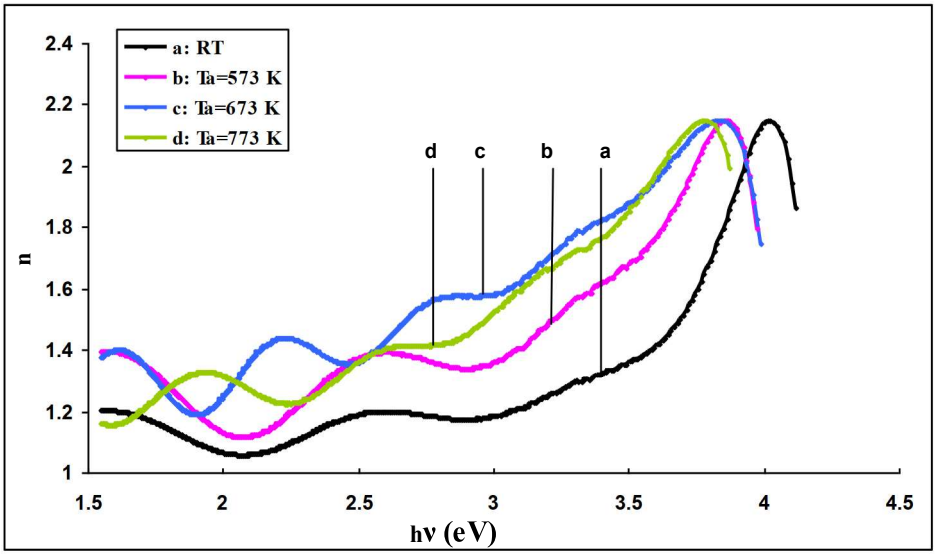

Fig. (4): Variation of n as a function of hυ for SnO_2 filmsat different annealing temperatures.

. The optical energy gaps for both allowed and forbidden direct transition have been calculated using Tauc equation, equation (5): [16]

$$(\alpha h\nu) = B(h\nu - E_g)^r \ldots\ldots(5)$$

Where B is Tauc constant and hυ is the photon energy, α is the absorption coefficient and r =1/2 for allowed direct transition and r =3/2 for forbidden direct transition as in figures (5),(6).The energy gap E_g of the samples was evaluated from the intercept of the linear portion of each curve with the hν..The obtained values of energy gap for different annealing temperatures are shown in table (3), Band gap lies in the range of (3.98-3.72) eV our results are in good agreement with those reported in literature [19].

The values of optical energy gaps as shown decrease with increasing annealing temperatures this may be attributed to the increase in the localizes levels near the band edges.

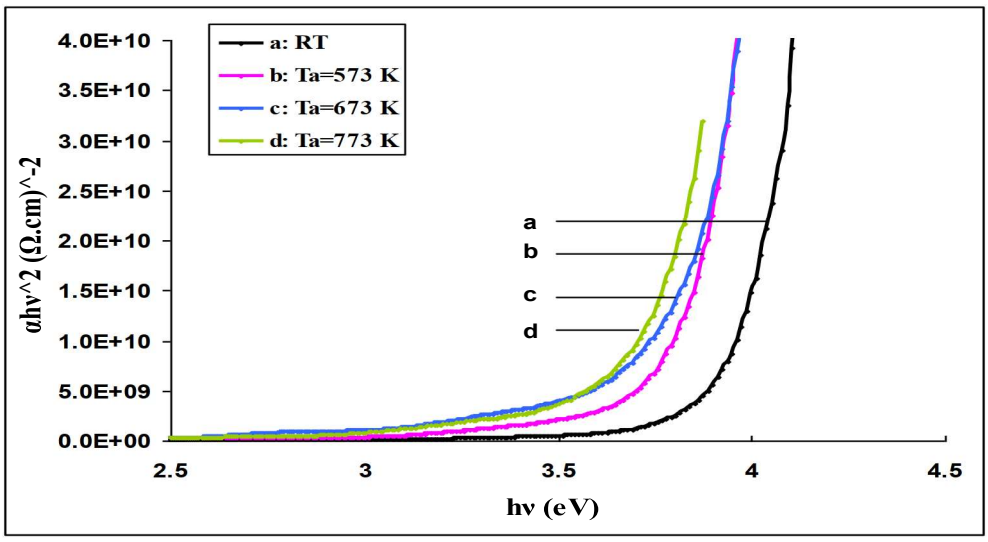

Figure (5). Variation $(\alpha h\upsilon)^2$ versus hυ for allowed direct transitionat different annealing temperatures.

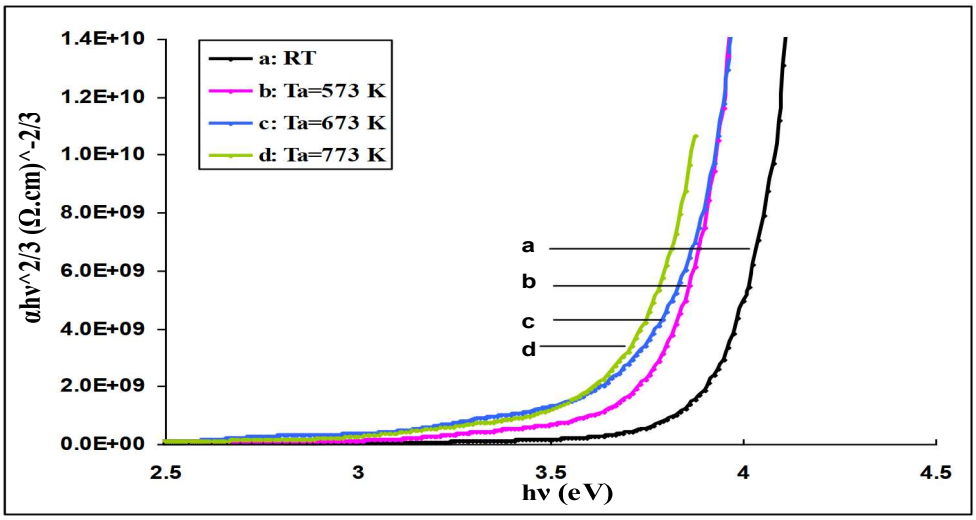

Figure (6). Variation $(\alpha h\upsilon)^{2/3}$ versus hυ for forbidden direct transition at different annealing temperatures.

In polycrystalline semiconductors where there are localized states in their energy gaps, the absorption edge becomes wide. The width of these localized states can be calculated by using Urbach rule [20],

$$\alpha = \alpha_o \exp\left(h\nu / E_u\right) \quad \text{.....(6)}$$

Where the tails width (E_u) is Urbach energy which is calculated from the slope of the plot between lnα and hν.as in figure (7). Our results are listed in table (3), which shows that (E_u) decreases with the increase of annealing temperatures (T_a). This effect can be explained as increasing of crystallites of films with annealing leads to a decrease in localized state.

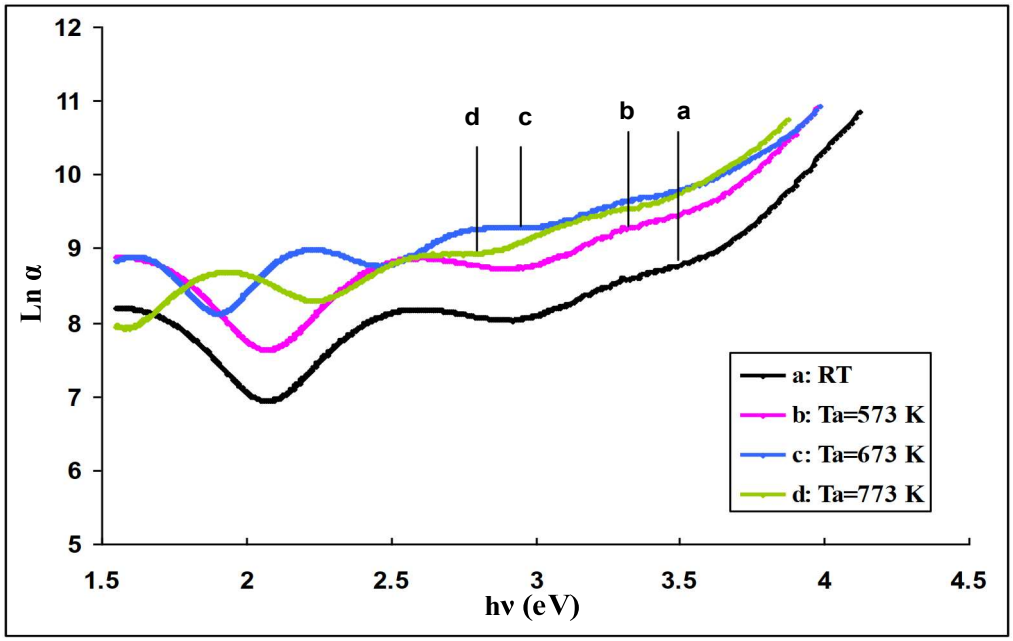

Figure (7). The variation of (ln α) versus hυ for SnO_2 thin films at different annealing temperatures.

Table (2): The values of energy gap for the allowed and forbidden direct transition at different annealing temperatures.

T_a (K)	E_u (Ev)	E_g (Ev)	
		Allowed	Forbidden
R.T	1.172	3.98	4
573	1.103	3.86	3.85
673	1.034	3.83	3.83
773	0.926	3.72	3.73

5. Conclusions:

There are main conclusions that have obtained from this work.

From X-ray diffraction results can be concluded that the structure of SnO_2 films is polycrystalline with tetragonal structure with preferential orientation in the (200) direction. Annealing process leads to improve in the crystallization.

From the optical properties concluded that the optical transitions in SnO_2 is direct transition and value of optical energy gap decreases with annealing temperature.

6. References:

[1] O.S. Heavens ,"Thin Film Physics", John Wily and Sons Inc , New York , (1973).

[2] R.Ueda and J. B. Millin ," Crystal Growth and Characterization ", Mc Graw-Hill , (1975).

[3] L.Eckortova ,"Physics of Thin Films", (plenum press), (1977).

[4] J.-K. Choi, I.-S. Hwang, S.-J. Kim, J.-S. Park, S.-S. Park, U. Jeong, Y.C. Kang, J.- H. Lee, Design of selective gas sensors using electrospun Pd-doped SnO_2 hollow nanofibers, Sensor. Actuator. B Chem. Volume 150, (2010),p.p 191–199.

[5] S. Das, V. Jayaraman, SnO_2: a comprehensive review on structures and gas sensors, Prog. Mater. Sci. Volume 66 (2014), p.p 112–255.

[6] Y. Bouznita,b, A. Hennic,* Characterization of Sb doped SnO_2 films prepared by spray technique and their application to photocurrent generation, Materials Chemistry and Physics Volume 233, 2019, p.p 242-248**.**

[7] K. Inyawilert, A. Wisitsoraat, C. Sriprachaubwong, A. Tuantranont, S. Phanichphant, C. Liewhiran, Rapid ethanol sensor based on electrolytically- exfoliated graphene-loaded flame-made In-doped SnO_2 composite film, , Sensors and Actuators B: Chemical, Volume 209, (2015), p.p40–55.

[8] G.O. Testoni, R.A.C. Amoresi, G.M.M.M. Lustosa, J.P.C. Costa, M.V. Nogueira, M. Ruiz, M.A. Zaghete, L.A. Perazolli, Increased photocatalytic activity induced by TiO_2/Pt/SnO_2 heterostructured films, Solid State Sci.Volum 76, (2018), p.p 65–73

[9] A. Tombaka, Y.S. Ocakb,c, F. Bayansald, Cu/SnO_2 gas sensor fabricated by ultrasonic spray pyrolysis for efective detection of carbon monoxide ,Applied Surface Science, Volume 493, (2019), p.p 1075-1082.

[10] HaoyuanXua,b,JianzhongLia,b,,YuFua,b,WenbinLuoa,b,YanwenTiana,b Deactivation mechanismandanti-deactivation modification of SnO_2-based catalysts for methane gas sensors, Sensors and Actuators B: Chemical ,Volume 299, (2019) ,P.126439.

[11] S.P. Choudhurya*, S.D. Gunjalb,c, N. Kumarid, K.D. Diwatee, K.C. Mohiteb, A. Bhattacharjeea Facile synthesis of SnO_2 thin film by spray pyrolysis technique and investigation of the structural, optical and electrical properties , materialstoday,Volum 3, Issue 6, (2016),P.P 1609-1619.

[12] K. Hu, F. Wang, H. Liu, Y. Li, W. Zeng, Enhanced hydrogen gas sensing properties of Pd-doped SnO_2 nanofibres by Ar plasma treatment, Materials Science, Ceramics International ,Volume 09, (2019), P.132.

[13] K. Bunpanga,b, A. Wisitsoraatc,d,e, A. Tuantranontc,e, S. Singkammof, S. Phanichphantc, C. Liewhirana,c,g, Highly selective and sensitive CH_4 gas sensors based on flame-spray-made Cr-doped SnO_2 particulate films, Sensors and Actuators B: Chemical, Volume 291, 2019, p.p177-191.

[14] Laifa Sang, Guogang Xu, Zhiwei Chen, Xinzhen Wang, Hongzhi Cui, Gaoyu Zhang, Yajie Dou Synthesis and characterization of Au-loaded SnO_2 mesoporous spheres by spray drying and their gas sensing property, Materials Science in Semiconductor Processing,Volume , (2020), P/ 104710.

[15] Qu Zhoua, Weigen Chenb, Lingna Xua,b, Rajesh Kumarc, Yingang Guia, Zhongyong Zhaoa, Chao Tanga, Shiping Zhua Highly sensitive carbon monoxide (CO) gas sensors based on Ni and Zn doped SnO_2 nanomaterials, Materials Science, Volume 44,(2018) 4392-4399.

[16] J.Taus, [Amorphous and Liquid Semiconductor] Plenums Press, New York and

London, 271, (1974).

[17] JCPDS-International Centre for Diffraction Data. All rights resaved ,PCPD Fwin Vol.1.30, card no. 36-1451.

[18] Radhyah Mahdi Shaker Jarrah, Effect of Substrate Temperature and Zn Additive toCdTe Thin Films on AC Mechanism and Cole-Cole Diagram, International Journal of Science and Research (IJSR), Volume 5 Issue 5, 2016, p.p1557-1563.

[19] A.Mohammed, M.Bagheri, D.Mohagheghi, M. Shokooh, Saremi, "The influence of Al doping on the electrical, optical and structural properties of SnO_2 transparent conducting films deposited by the spray pyrolysis technique", J. Phys. D. Appl. Phys., Volume 37, (2004), p.p. (1248-1253).

[20] F. Urbach, P hys. Rev., 92 (2006) 1324.